

# *Genetic Indices in Hyperpycnal Systems: A Case Study in the Late Oligocene–Early Miocene Merecure Formation, Maturin Subbasin, Venezuela*

**Carlos Zavala**

*GCS Argentina, Universidad Nacional del Sur, Bahía Blanca, Argentina*

**Jose Marcano, Jair Carvajal, and Manuel Delgado**

*Petróleos de Venezuela Sociedad Anónima (PDVSA), Laboratorio Geológico El Chaure, Puerto La Cruz, Venezuela*

## **ABSTRACT**

The mapping and analysis of ancient turbidite deposits using geographically dependent sedimentologic indices (or proximity) determined by genetic facies relationships and grain-size variations were mostly applied during the early years of turbidite research. Nevertheless, the understanding that fine-grained deposits (thin-bedded turbidites) can also occur in proximal (interchannel) areas, and the impossibility of differentiating them from real distal deposits, revealed many inconsistencies in this approach to the development of turbidite fan facies models. More recently, a genetic facies tract has been proposed for hyperpycnal systems, which distinguishes between thin-bedded deposits accumulated in interchannel areas from those deposited on distal areas.

The genetic facies tract proposed for hyperpycnal systems in marine settings comprises three main facies categories related to bed-load, suspended-load, and lofting processes, respectively. Bed-load-related facies are coarse grained and related to drag forces provided by the overpassing turbulent flow. Suspended-load-related facies are composed of fine-grained sandstones and originate from the gravitational collapse of the suspended load as the long-lived flow progressively wanes. Lofting-related facies are the result of the fallout of very fine-grained sands,

silts, plant debris, and micas from lofting plumes mainly in flow-margin areas. Proximal (Pt) and lateral (Lt) facies indices have been defined based on the relative abundance of B, S, and L facies within a stratigraphic interval. The Pt and Lt indices are dimensionless numbers that range from 100 to 0. The Pt index measures how proximal a given stratigraphic section is with respect to the entire hyperpycnal system. The Lt index provides an indication of the stratigraphic lateral distance of a given section with respect to the flow axis. These genetic indices were applied to hyperpycnal deposits of the late Oligocene–early Miocene Merecure Formation, Maturín Subbasin, Venezuela.

Results suggest that the Merecure Formation may be more extensive than previously considered with a main sediment source from cratonic areas located in the south and southeast. Index mapping also suggests a syntectonic accumulation during the Oligocene, which controlled the subaqueous topography and, thus, the distribution of sand bodies.

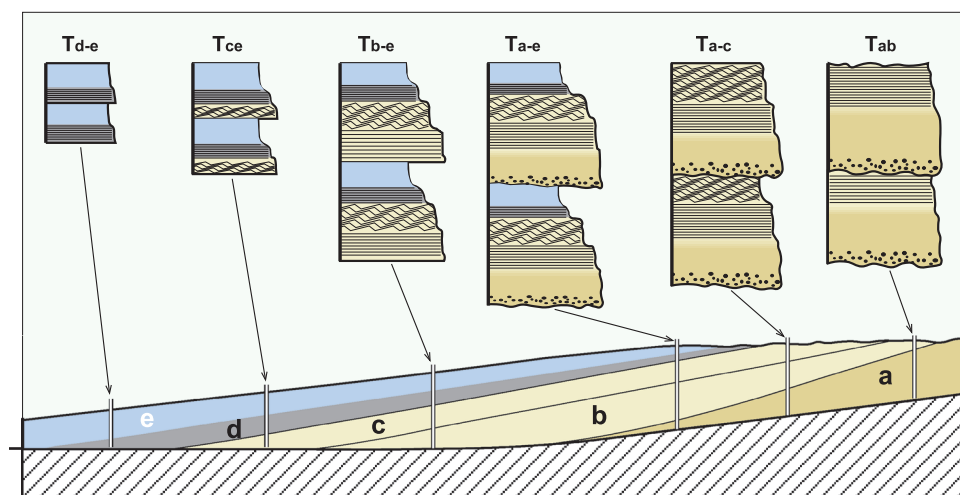
## INTRODUCTION

The fact that turbidites change facies with an associated decreasing grain size from source to the basin was known early in turbidite research (Natland and Kuenen, 1951). The recognition and analysis of the grain size, depositional features, and facies types considered as typical of proximal to distal settings led to establishing several guidelines aimed at distinguishing between proximal and distal turbidites. During the 1960s, many attempts were made to quantify these facies and associated textural changes, which led to the proposal of the proximity index (P index) in the analysis of turbidite deposits (Walker, 1967). The P index analysis was applied with some early success, but the understanding that fine-grained turbidites could also occur in interchannel (levee) proximal areas led to confusing interpretations. The description of fine-grained proximal deposits resulted in the progressive abandonment of the P index analysis, which was replaced by facies analysis (Mutti and Ricci Lucchi, 1972). The controversy over the origin of fine-grained facies in turbidite deposits resulted in the concept of thin-bedded turbidites, which was far more descriptive and not directly dependent on its position in a proximal-to-distal profile.

In recent years, the increased understanding that many turbulent flows in the marine setting could originate by direct discharge from rivers in flood (or hyperpycnal flows; Bates, 1953; Normark and Piper, 1991; Mulder and Syvitski, 1995; Mutti et al., 1996, 1999) has opened a new research frontier in shelfal to deep-marine clastic sedimentation. Hyperpycnal flows and their deposits, hyperpycnites (Mulder et al., 2003), originate when rivers discharge a turbulent mixture of water and sediment having a bulk density that

exceeds that of water in the receiving basin (Bates, 1953). In the case of a river flow entering a marine basin, the fluvial discharge should have a suspended-load concentration exceeding 35 to 45 kg/m<sup>3</sup> to overcome the density contrast between fresh water and seawater (Mulder and Syvitski, 1995). This land-generated and relatively dense flow will sink in coastal areas, generating a turbulent flow that moves basinward along the bottom of the basin, allowing the transfer of a large volume of fresh water and sediments from the river to the basin floor. Depending on different hydrologic and physiographic factors, hyperpycnal flows can develop either in the shelf or in deep-water settings, and their deposits can be considered as true shelfal (see also the concept of shelfal sandstone lobes in Mutti et al., 1996) to deep-water turbidites. Hyperpycnite beds related to sustained flows in marine settings can be recognized by some common and distinguishing characteristics such as reverse-normal grading (Mulder et al., 2003), gradual facies recurrence (Zavala et al., 2006a), abundant plant debris (Plink-Björklund and Steel, 2004), and associated silt-sand couples with abundant plant debris and mica known as lofting rhythmities (Zavala et al., 2006c, 2008b).

Recently, a new genetic facies tract was proposed for the analysis of hyperpycnal deposits in lacustrine to marine settings (Zavala et al., 2006b, 2011; Zavala, 2008). This facies tract classifies hyperpycnal-related facies according to the main processes active during the accumulation of hyperpycnites, from bed load (facies B), suspended load (facies S), and lofting (facies L). Bed-load facies accumulate in proximal areas because of shear forces provided by the overpassing turbulent flow, whereas L facies mainly develop at flow-margin (levee) areas. Suspended-load facies, however,



**FIGURE 1.** Variations in the typical Bouma facies sequence in a downcurrent direction (from right to left). Note that in proximal facies sequences, the upper intervals are missing (Tc–Te), whereas distal turbidite beds progressively lose the lower intervals (Ta–Tb). These facies changes in the basinward direction can be used to predict the occurrence of certain facies types in a given area. Modified after Bouma, 1962.

are related to the progressive collapse and accumulation of turbulent-suspended materials when the flow progressively wanes in medium to distal areas. Consequently, quantifying the relationship between these three categories of genetically related facies allows determination of the position of a given hyperpycnite section within the entire depositional system. This geographically oriented analysis is possible by the determination of two partially dependent genetic indices, termed proximal (Pt) and lateral (Lt) facies indices. The Lt index solves the interpretation problem of relatively low Pt of levee areas that was encountered in the earlier studies of turbidite deposits (Macdonald, 1986).

This chapter provides an example of this new methodology applied to a subsurface study conducted in the Oligocene–early Miocene Merecure Formation, located in the Maturin Subbasin, Venezuela. Because the Merecure Formation is one of the main oil-bearing units of eastern Venezuela, this methodology has substantially improved the facies analysis in the prediction of distribution and quality of clastic reservoirs.

## INDICES (PROXIMALITY) IN TURBIDITE STUDIES

### *General Overview*

When Natland and Kuenen (1951) first documented that the Ventura Basin (California) turbidite beds thinned in a downcurrent direction, several attempts were made to quantify the main characteristics of proximal-to-distal facies in turbidites. Bouma (1962) published perhaps the most famous facies sequence in the Peira Cava flysch (Oligocene) composed of five divisions, termed Ta to Te. The divisions form a fining-

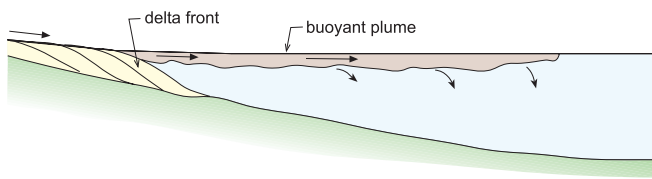
upward sequence with a basal, massive, and graded sandstone (Ta) that is overlain by parallel-laminated sandstones (Tb) and fine-grained rippled sandstones (Tc), and capped by silts and hemipelagic mud (Td and Te). Bouma (1962) also noted that in a proximal setting, the facies sequence tends to lack the upper divisions, whereas toward the distal setting, the basal intervals are progressively absent (Figure 1). This sequence was quantified by Walker (1967), who defined a P index based on the percentage of beds within a group of beds that began with a particular Bouma division. According to Walker (1967), the P index can range from 100 (most proximal) to 0% (most distal) and could be used to estimate the location of any given section relative to its source direction.

The concept of proximity in turbidite deposition was supported by the premise that a turbidity current tends to lose energy with distance along its travel path, accounting for the basinward decrease in erosion and the deposition of progressively finer grained sediments. Although the idea of depletive flows (in the sense of Kneller and Branney, 1995) in turbidity currents is valid, flows in proximal areas are commonly channelized and exhibit a strong lateral anisotropy in flow velocity that results in the accumulation of fine-grained deposits in flow-margin areas (levee deposits) having similar characteristics to those accumulated in distal areas (Haner, 1971; Mutti and Ricci Lucchi, 1972). These inconsistencies were discussed in several subsequent articles (Lovell, 1969, 1970; McCabe and Waugh, 1973) that demonstrated the P index is a poor guide to proximity.

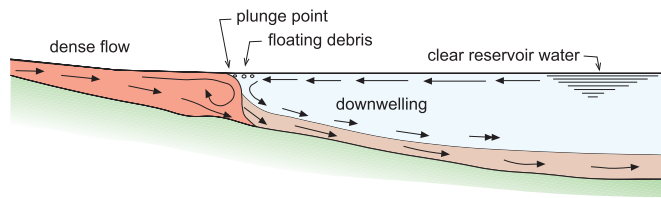
The increased understanding of internal characteristics of turbidite fan models revealed that fine-grained deposits can develop in different fan settings, and consequently, many authors suggested that

**A) Hypopycnal flow**

(inflow water density &lt; basin water density)

**B) Hyperpycnal flow**

(inflow water density &gt; basin water density)



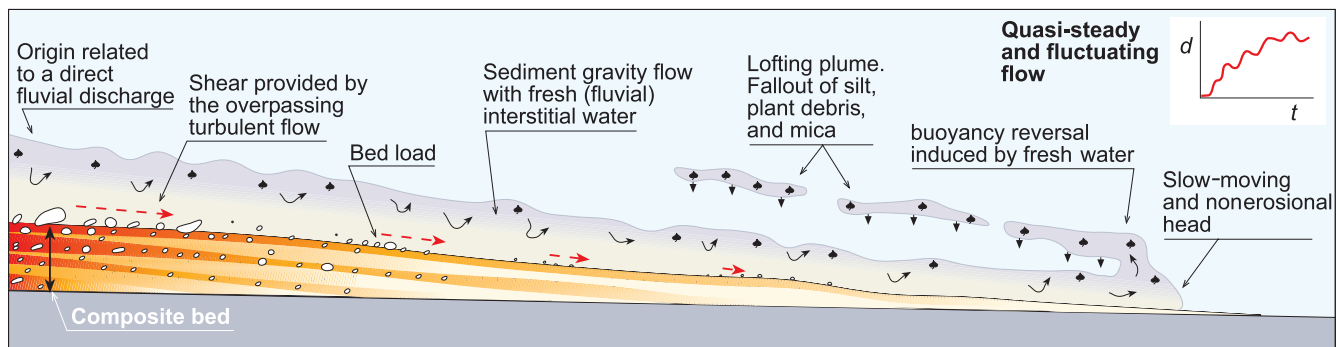
**FIGURE 2.** Comparison between (A) hypopycnal and (B) hyperpycnal flows (original concept by Bates, 1953). Note that in the case of the hyperpycnal flow, the fluvial discharge sinks beneath the less dense water body, continuing its travel basinward as a quasi-steady underflow. Panel B was redrawn from the pioneer work of Knapp (1943). After Zavala et al. (2008a).

the terms “proximal” and “distal” should be avoided (Nelson et al., 1978) for facies classifications, and all fine-grained sediments should be considered as thin-bedded turbidites without any implication for proximal or distal setting (Walker, 1978; Nilsen, 1980). Consequently, modern use of the terms proximal or distal turbidites refers only to the distance from the source area and should not be used to describe facies, the characteristics of which can sometimes be controversial (Macdonald, 1986).

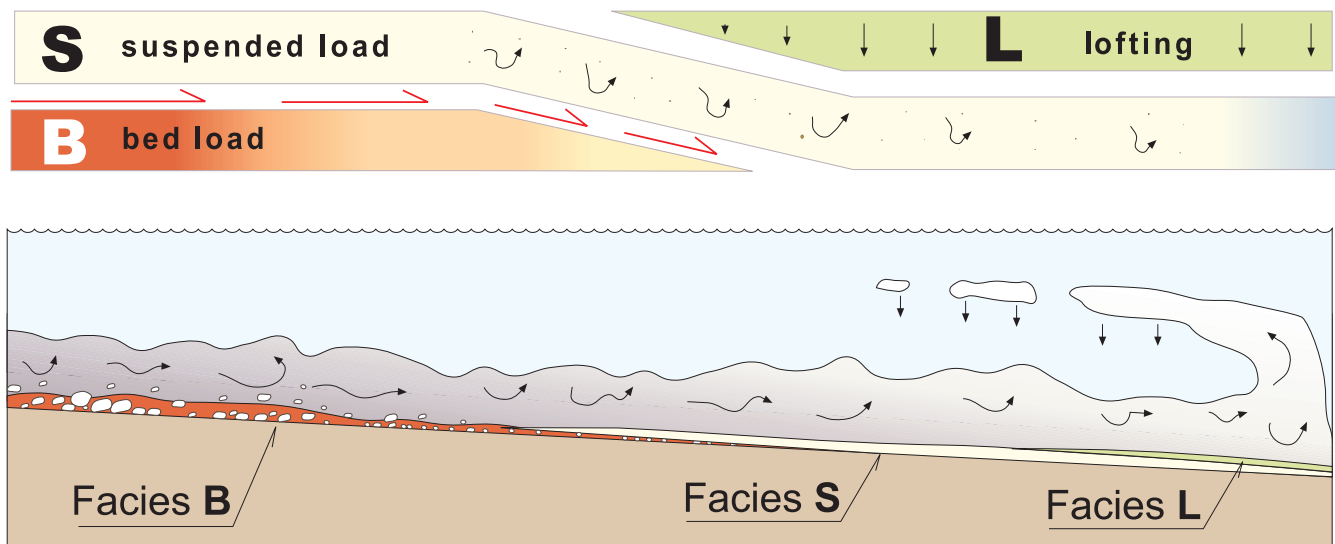
### ***Genetic Facies Tracts and Hyperpycnal Sedimentation: Hyperpycnal Systems***

Recent advances in the understanding of a relatively new category of depositional system, termed “hyperpycnal system” (Zavala et al., 2006a), offer new perspectives to understanding the distribution of shelfal to deep-water sandstone strata. A hyperpycnal system is the subaqueous extension of the fluvial system (the fluvial system in the sense of Schumm, 1977, 1981) and originates when a river in flood discharges a relatively dense turbulent mixture of fresh water

and sediment with a bulk density that exceeds that of the receiving water body (Mulder and Alexander, 2001). When these fluvial-derived dense flows reach the coast, they plunge to the sea floor and move basinward as a sustained and quasi-steady turbulent flow (Figure 2B). If the hyperpycnal flow can be maintained for a long period of time, these flows have the capacity to travel hundreds of kilometers basinward (Nakajima, 2006; Cheng-Shing and Ho-Shing, 2008; Bourget et al., 2010) even in relatively low gradient settings and to deposit very thick successions, especially in topography-controlled depocenters. Hyperpycnal system deposits commonly show some characteristic patterns erroneously considered as typical of fluvial deposition, including bed load, channelization, and meandering (Cheng-Shing and Ho-Shing, 2008). Contrary to conventional models for turbidity current sedimentation (Mutti et al., 1999, 2009), coarse-grained materials are not transported at the head in long-lived hyperpycnal flows but are transported as bed load (Figure 3) because of shear forces provided by the overpassing turbulent flow



**FIGURE 3.** Main characteristics of long-lived hyperpycnal flows and their typical deposits. The complexity of the river (outflow) hydrograph (drawn on the right upper corner) results in the accumulation of composite beds (Zavala et al., 2007a).  $d$  = discharge;  $t$  = time.



**FIGURE 4.** Conceptual diagram for facies analysis of hyperpycnal deposits with associated bed load in marine settings. Facies B includes all those facies related to bed-load processes developed at the base of an overpassing long-lived turbulent flow. Facies S corresponds to the gravitational settling of sand-size materials transported in suspension by the turbulent flow (suspended-load facies). Facies L is related to the fallout of fine-grained materials lifted into the interstitial fresh water contained in the flow once its sand-size suspended load is deposited. After Zavala et al., 2006b, 2011; Zavala, 2008.

(Plink-Björklund and Steel, 2004; Zavala et al., 2006b; Zavala, 2008).

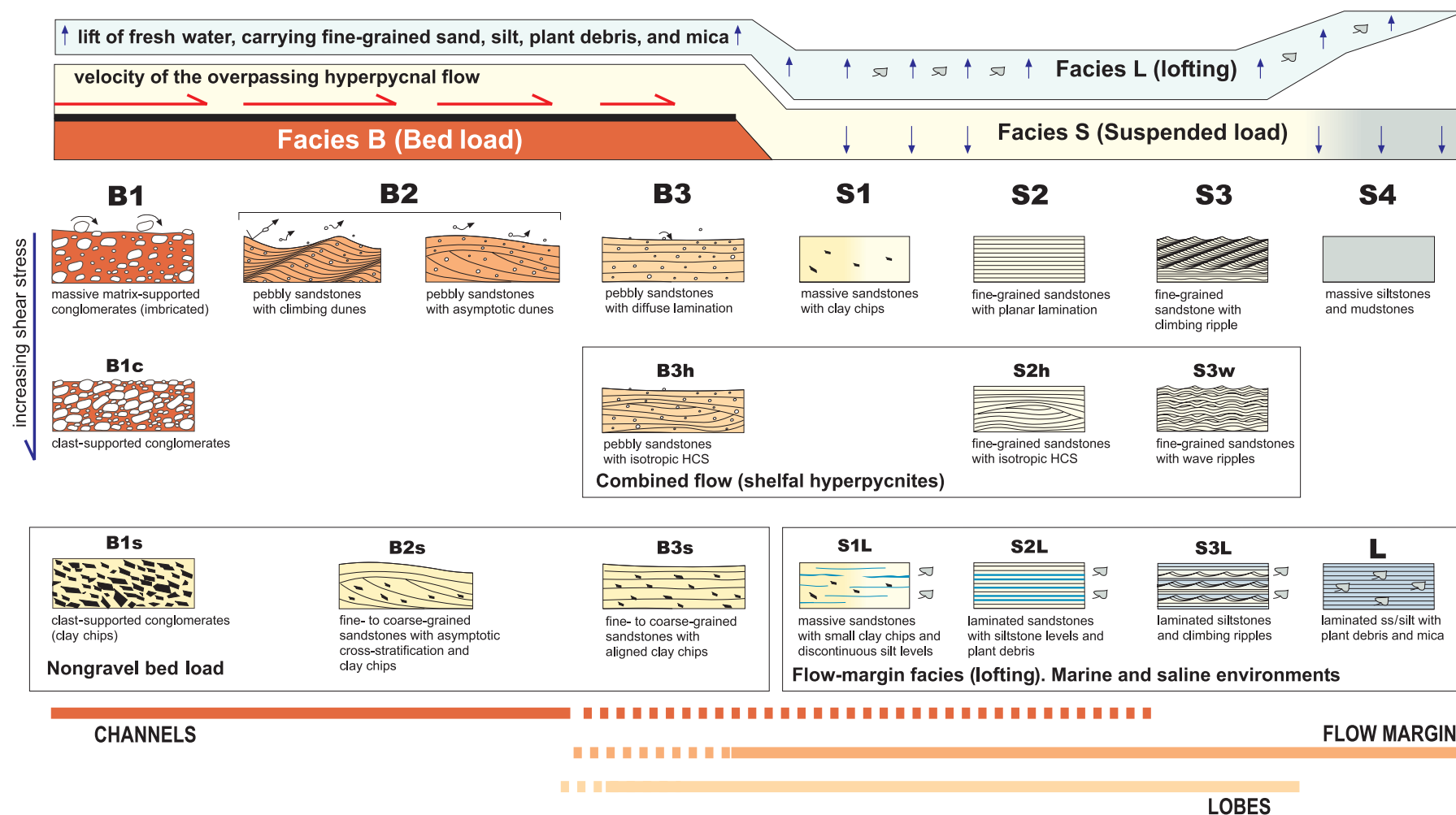
#### ***Facies Analysis of Hyperpycnal Systems: A Genetic Approach***

The basic scheme of facies classification in this chapter has been applied and tested during the last 7 yr in several hyperpycnal stratigraphic units (Zavala et al., 2006b, 2011; Zavala, 2008). This facies classification is based on the distinction of three main categories of genetic facies, related to bed-load (facies B), suspended-load (facies S), and lofting (facies L) processes (Figure 4).

Facies B (bed load) includes the coarsest sediments of the facies tract that are transported by drag and shear forces provided by the overpassing turbulent hyperpycnal flow. Consequently, B facies are dominant in proximal positions. Three main facies types are recognized in this category (Figure 5), termed B1 (massive conglomerates), B2 (pebbly sandstone with asymptotic low-angle cross-stratification), and B3 (pebbly sandstone with diffuse planar lamination). Facies S is fine grained and is deposited because of the gravitational collapse of turbulent suspended load in the main body of the hyperpycnal flow. Four facies types are recognized within this category (Figure 5), termed S1 (massive sandstone), S2 (laminated sand-

stone), S3 (sandstone with climbing ripples), and S4 (massive siltstone and mudstone). Facies L (lofting) accumulates from a lofting plume, which is a typical feature of hyperpycnal inflows in marine or saline environments. In this situation, the hyperpycnal discharge contains a fluid (fresh water) that is less dense than ambient seawater. Consequently, when the flow progressively loses parts of its suspended load by deposition, the current will lift from the substrate through buoyancy reversal (Sparks et al., 1993; Kneller and Buckee, 2000; Hesse et al., 2004), forming lofting plumes charged with fine-grained sediments, plant debris, and micas. These fine-grained sediments are gradually deposited on the sea bottom, forming repeated silt-sand couplets of great lateral extent known as lofting rhythmites (Zavala et al., 2006c, 2008b). Individual sand-silt levels in lofting rhythmites are commonly up to 2 mm (0.08 in.) thick and show good lateral continuity. Silt-sandstone couplets and their intercalations integrate laminated and decimeter-thick packages. These laminated packages lack or show rare and poorly diverse ichnofaunas. Lofting rhythmites appear isolated between mudstone successions or located between or toward the top of massive-to-laminated tabular sandstone beds. The recognition of lofting facies in marine environments is therefore extremely important because it allows the diagnosis of a direct fluvial connection and a hyperpycnal origin





**FIGURE 5.** Conceptual scheme for the genetic interpretation of clastic facies in hyperpycnal systems. Type B facies relates to bed-load processes at the base of an overpassing long-lived turbulent flow. Type S facies originate from the gradual accumulation of sand-size suspended materials carried in the turbulent flow. Facies L is composed of very fine-grained sandstones interbedded with laminated silts with abundant plant debris and mica deposited by fallout from a lofting plume. Facies L is exclusive of marine/saline environments. After Zavala et al., 2006b, 2011; Zavala, 2008. HCS = hummocky cross-stratification; ss/silt = sandstone/silt.

for associated deposits. Lofting rhythmites should not be confused with tidal rhythmites. Some distinguishing characteristics of lofting rhythmites include (1) lack of true mud couplets—the separating levels between sand-silt intervals are composed of plant debris and micas instead of mud; (2) absence of clear internal organization in neap-spring cycles; (3) close association and transitional (lateral) gradation with massive (facies S1L), laminated (facies S2L), and rippled (facies S1L) sandstones; (4) lack or very scarce bioturbation dominated by *Palaeophycus*; (5) well-developed normal grain-size grading in individual laminae (Zavala et al., 2008b).

Because the hyperpycnal flows show a drastic velocity decrease from the flow axis toward the laterals (Zavala et al., 2006a), facies L will be mainly accumulated in flow-margin (levee) areas.

Hyperpycnites commonly compose very complex beds showing internal erosional surfaces and gradual facies recurrences related to deposition from long-lived and highly dynamic fluctuating flows (Zavala et al., 2006a; Lamb et al., 2008; Jackson and Johnson, 2009; Lamb and Mohrig, 2009). This complex behavior results in the accumulation of composite beds (Figure 3) (Zavala et al., 2007a) having an internal facies arrangement that strongly departs from conventional facies models deposited from surge-like turbidity flows (Bouma, 1962; Mutti et al., 2003).

Facies B characterizes transfer zones, and its occurrence allows prediction of sandstone deposits (facies S) basinward. Facies L are mostly developed in marginal flow areas.

### **Genetic Indices: Proximal and Lateral Facies Indices**

The genetic-oriented analysis applied to the study of hyperpycnal systems allows facies mapping and recognition of bypass, depositional, and marginal areas in the subsurface. Two main indices were considered in this study, termed proximal (Pt) and lateral (Lt) facies indices (Zavala et al., 2007b, 2008a). These indices should be calculated individually for each analyzed section.

#### **The Proximal Facies Index**

The Pt index is a dimensionless number that measures how proximal a given hyperpycnal sediment body is with respect to the entire hyperpycnal system. The Pt index is based on the relative dominance of bed-load-related facies (B facies) in proximal po-

sitions and the basinward increase of suspended-load facies (S facies) as the long-lived hyperpycnal flow progressively wanes with the subsequent collapse of suspended materials. The Pt index is calculated as follows:

$$Pt = 100B/(B + S) \quad (1)$$

where Pt is the proximal facies index, B is the total thickness of bed-load facies, and S is the total thickness of suspended-load facies in a given stratigraphic section or core. Note that this analysis only applies for hyperpycnal facies.

The Pt index is a dimensionless number that ranges between 0 and 100. The greater the Pt index, the more proximal the deposit is with respect to its source area. Proximal indices between 100 and 50 characterize proximal parts of the system. Proximal indices between 50 and 0 suggest intermediate positions in the system. A proximity of 0 marks the end of the channel-lobe transition zone (CLTZ) (Mutti and Normark, 1987; Wynn et al., 2002) and the beginning of the distal part of the system (lobe) with tabular sandstone beds almost entirely composed of S facies. In addition, the decay rate of the Pt index between different locations can be used as a proxy to estimate the dimensions of the hyperpycnal system under consideration.

#### **The Lateral Facies Index**

The Lt index is a dimensionless number that ranges from 0 to 100, which is a measure of the relative abundance of L facies with respect to B and S facies in a given sedimentary section. In other words, the Lt index will give an indication of the relative lateral location of the analyzed well or outcrop from the main flow axis, which will be dominated by B or S facies. The lateral facies index can be obtained as follows:

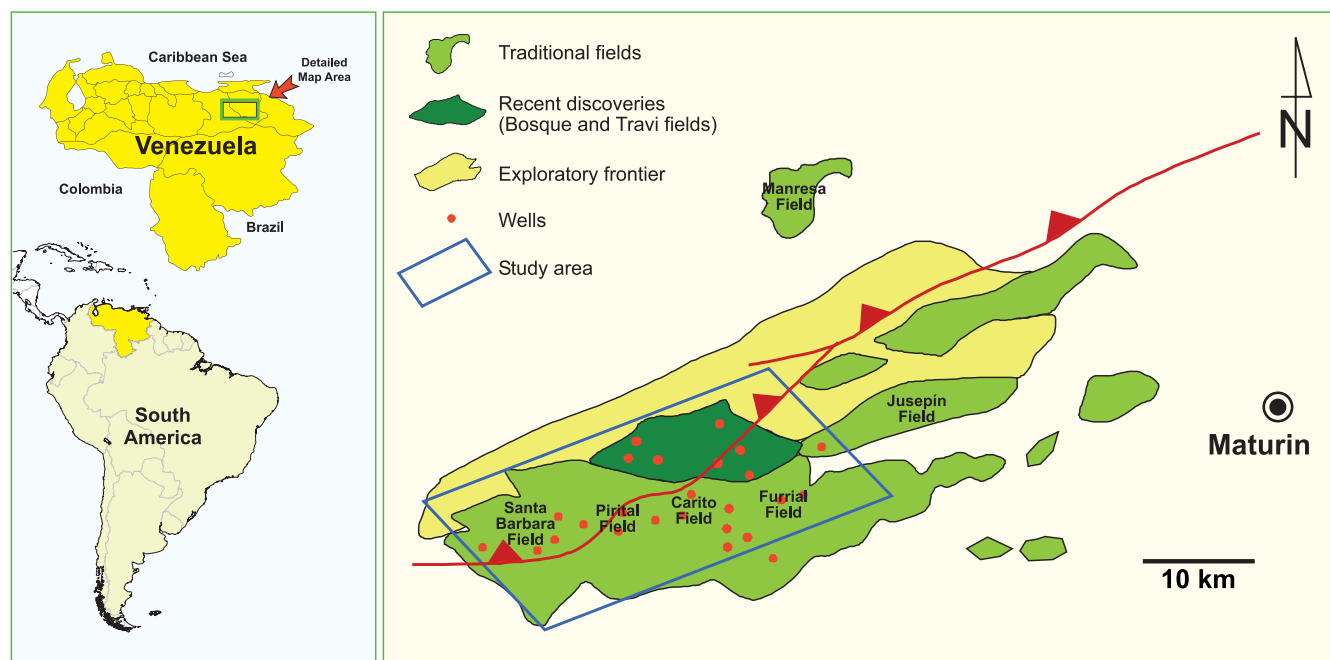
$$Lt = 100L/(L + B + S) \quad (2)$$

where Lt is the lateral facies index, L is the total thickness of lofting facies, B is the total thickness of bed-load facies, and S is the total thickness of suspended-load hyperpycnal facies in an analyzed core or outcrop.

A hyperpycnal flow is a sediment gravity flow, and the accumulation of coarse-grained facies will be very sensitive to any subaqueous topography. Facies B and S tend to develop infilling the lowermost positions of the submarine landscape. On the contrary, L facies mostly characterizes relatively elevated (levee)

Juana et al., 1980; Campos et al., 1985), (2) estuarine to shallow-marine deposits (Porrás et al., 2002), and more recently (3) shallow (shelfal) hyperpycnal systems (Zavala et al., 2007b). The hyperpycnal interpretation of the Merecure Formation is derived from careful conventional facies analysis of two cores located in the Travi and Santa Barbara fields. Main observations that support this interpretation are as follows: (1) the common occurrence of very thick (>5 m [16 ft]) massive and laminated sandstones showing gradual vertical facies changes and facies recurrence, which suggest an accumulation from long-lived fluctuating turbulent flows (Zavala et al., 2006a; Lamb et al., 2008; Jackson and Johnson, 2009; Lamb and Mohrig, 2009); (2) the association of these coarse-grained facies with lofting rhythmites with abundant plant debris and mica, which are considered diagnostic features of marine hyperpycnal deposition (Zavala et al., 2006c, 2008b); and (3) the associated occurrence of upper bathyal foraminifers (Delgado, 2007, personal communication), which support a relatively deep fully marine environment. Abundant plant debris locally showing entire leaves is also considered to be evidence of a direct fluvial connection (Plink-Björklund and Steel, 2004; Petter and Steel, 2005; Zavala et al., 2006a).





**FIGURE 7.** Location map of the Maturin area showing the study area and main oil fields.

This chapter provides an example of sedimentologic indices analysis applied to the Oligocene-early Miocene Merecure Formation in the northern part of the Monagas state, Venezuela. A total thickness of 3876.75 m (12,718.99 ft) of core was described and integrated with electrical logs. Facies description and classification was done according to the genetic facies scheme proposed for hyperpycnal deposits (Zavala et al., 2006b, 2011; Zavala 2008).

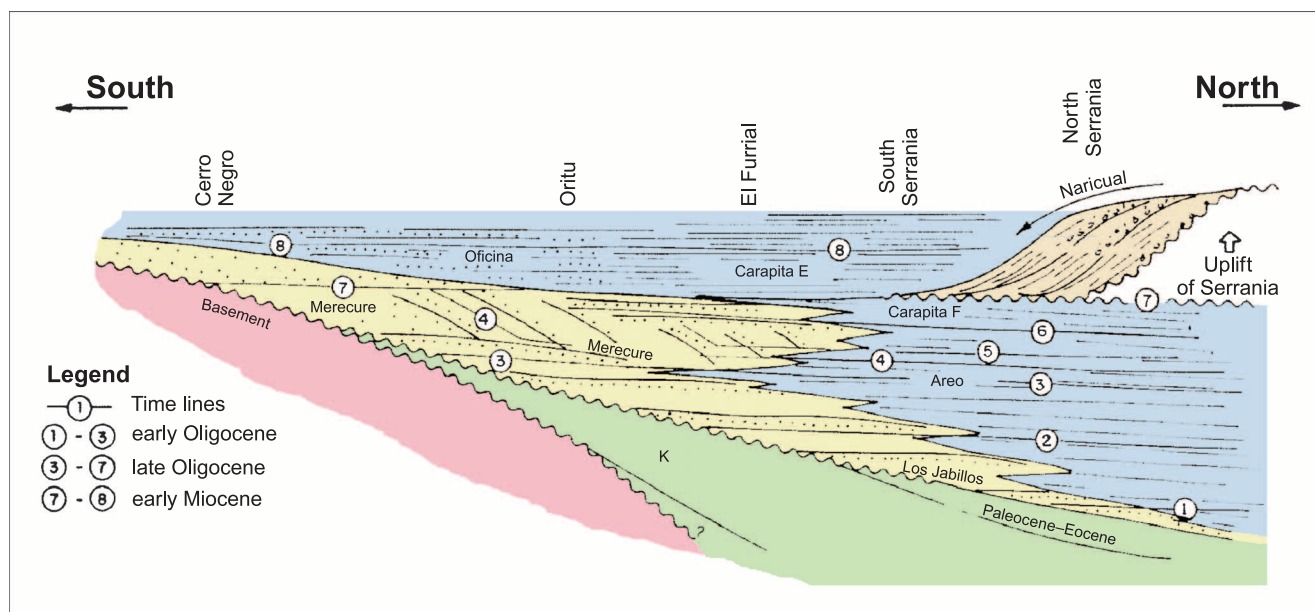
### ***Geological Framework***

The study area covers approximately 1000 km<sup>2</sup> (386 mi<sup>2</sup>) and is located within the Maturin Sub-basin, which forms the eastern part of the eastern Venezuela Basin (Figure 7). The sedimentary fill of this basin consists of about 9000 m (29,500 ft) of marine and continental deposits accumulated in a passive margin setting (Cretaceous–Eocene) followed in post-Eocene by a compressive foreland basin (Erich and Barrett, 1994) related to the oblique collision of the Caribbean plate against the South American plate. This oblique collision zone migrated progressively eastward during the late Oligocene–earliest Miocene, dividing the foreland basin into three areas: (1) a southern platform area, (2) a central foredeep, and (3) a northern region overthrust area (Parnaud et al., 1995).

As a consequence of major foreland basin subsidence, a very thick succession of clastic sediments

accumulated during the Oligocene and Miocene following a roughly east-west elongate depocenter. These clastic deposits consist of a basal coarse-grained succession (Merecure Formation) followed in sharp contact with deep-marine fine-grained accumulations (Carapita Formation). The Merecure Formation is composed of up to 500 m (1640 ft) of alternations of fine- to coarse-grained sandstones and shales. These sandstones of the Merecure Formation grade northward into a fine-grained succession (Areo Formation), interpreted as outer-shelf deposits (Stainforth, 1971; Parnaud et al., 1995). These clastic deposits were mostly sourced from the cratonic Guyana shield located to the south (Schlumberger, 1997). The Merecure Formation is partially equivalent to the Naricual Formation (Socas, 1991), which corresponds to coarse-grained deposits supplied from the north that accumulated close to an early uplifted and deformed mountain front or “serrania” (Figure 8) (Parnaud et al., 1995).

Detailed analysis of well logs and regional correlation of more than 50 wells allowed interpretation of a sequence-stratigraphic framework for the upper Oligocene–lower Miocene deposits in the area. A total of three main depositional sequences (M1, M2, and M3) were recognized and correlated. Each sequence is composed of an overall thinning and fining-upward lithogenetic unit (Figure 9). Each major sequence is in turn composed of up to three lower hierarchical elementary sequences. Main depositional sequences



**FIGURE 8.** Conceptual regional cross section showing the deposition of Oligocene and early Miocene sediments. After Parnaud et al. (1995). K = Cretaceous.

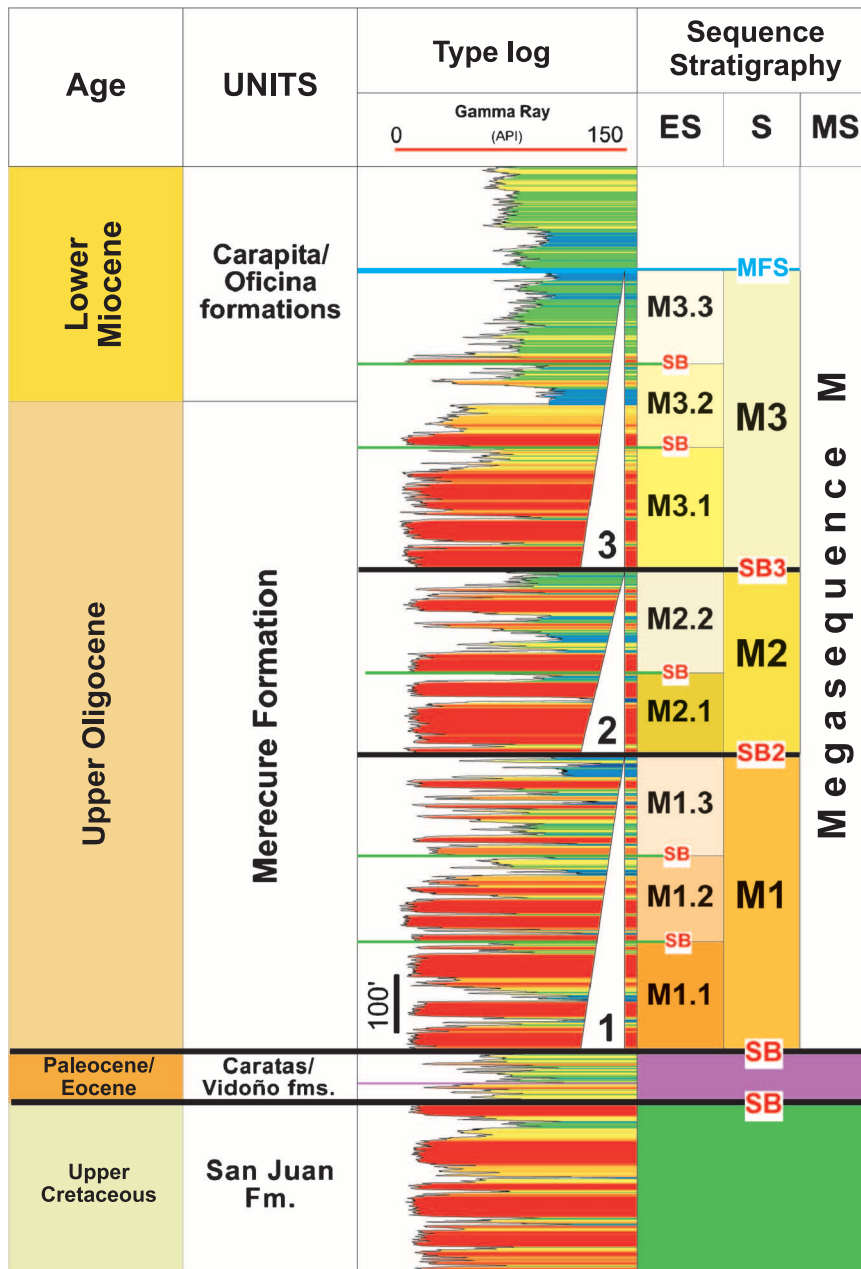
start with thick deposits of medium- to coarse-grained sandstones, which evolve upward into intercalated siltstones and fine-grained sandstones, ending with massive and bioturbated mudstones. The definition of the hierarchical framework of bounding surfaces was applied in this chapter to build the basic sequence-stratigraphic schema derived from a log analysis of the internal cyclicity complemented by core analysis. In the Merecure Formation, main sequence boundaries seem not to be related to relative changes in sea level because no evidence of subaerial exposure or shallow-water indicators was found above sequence boundaries. Major sequence boundaries commonly develop over Glossifungites ichnofacies and are in turn marked by a drastic increase in the grain size and thickness of sandstone bodies. These characteristics suggest a highly variable and cyclically ordered sediment yield to the basin via hyperpycnal flows, possibly controlled by climatic and tectonic cycles (Mutti et al., 2009).

### ***The Merecure Formation: Facies Analysis***

A regional subsurface study of core and well log data from 30 wells over an area of 1000 km<sup>2</sup> (386 mi<sup>2</sup>) reviewed the origin, stratigraphy, and sediment distribution of the Merecure Formation. As previously discussed, the origin of the Merecure Formation has been related to brackish to open marine conditions in fluvial-deltaic (González de Juana et al., 1980; Campos

et al., 1985) to estuarine shallow-marine environments (Porras et al., 2002), although no detailed facies analysis or diagnostic features were provided to support these interpretations. In the study area, core data lack evidences of coastal to shallow-marine structures such as tidal bundles, root marks, desiccation cracks, or extensive-wave reworked strata. Most sand bodies (>80%) are composed of massive or crudely stratified beds, evidencing an origin mainly related to sustained long-lived turbulent (sediment gravity) flows (Kneller and Branney, 1995; Zavala et al., 2007b, 2008a; Sumner et al., 2008). These deposits are associated with outer neritic to upper bathyal marine fauna (Campos et al., 1985) and abundant plant remains.

A total of 3876.75 m (12,718.99 ft) of core were described and analyzed in detail, from which 13 sedimentary facies were defined (Figure 10). Main facies include massive to cross-stratified pebbly sandstones that grade basinward into massive to laminated fine-grained sandstones. With the only exception of facies P, which is related to shelfal accumulation under nonflood conditions, all other recognized facies are associated with hyperpycnal flow discharges. Facies classification was done using the genetic and predictive facies analysis of hyperpycnal systems (Figure 3) (Zavala et al., 2006b, 2011; Zavala, 2008). The 12 hyperpycnal facies types can in turn be grouped into B, S, and L processes and deposits. The characteristics of the identified facies are summarized in Figure 10, together with their average porosity.



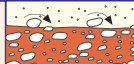
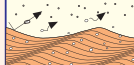
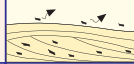
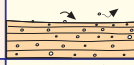
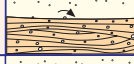
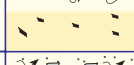

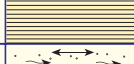

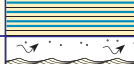

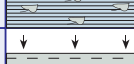

**FIGURE 9.** Type log of the Merecure Formation with proposed sequence stratigraphy. The 100-ft (30-ft) scale bar was indicative. ES = elementary sequence; MFS = maximum flooding surface; MS = megasequence; S = sequence; SB = sequence boundary; Fm. = Formation.

The B-type facies category includes coarse-grained sandstones and fine-grained conglomerates with abundant sandstone matrix. Main facies types of this category are massive (facies B1; Figure 11A, B), low-angle cross-bedded (facies B2; Figure 11C, D), and roughly laminated (facies B3; Figure 11E, F) coarse-grained deposits, commonly composing thick beds showing gradual and recurrent facies changes.

The S-type facies category is composed of fine-grained sandstones. Main types of S facies include massive (facies S1; Figure 12A, B), laminated (facies S2), and rippled (facies S3) deposits. Massive sandstones are very common, typically displaying isolated

*Ophiomorpha* and *Thalassinoides* burrows related to doomed pioneers (Grimm and Föllmi, 1994). Laminated sandstones commonly show small-scale hummocky cross-stratification (HCS) (facies S2h; Figure 12C), which suggest combined flow conditions in shelfal areas.

The L-type facies category (Figure 12E–G) is the result of the fallout of very fine-grained sands, silts, plant debris, and micas from lofting plumes mainly in flow-margin areas. The transition from the flow axis to flow margin is characterized by massive sandstone beds interbedded with beds containing abundant plant debris (facies S1L; Figure 12D).

Facies			Lithology	Sedimentary Structures	Origin	Thickness (m)	Porosity
							01020
Bed Load	B1		Matrix-supported fine-grained conglomerates	Massive, clay chips	Bed load related to the overpassing of long-lived turbulent flows	0.1 – 0.9	8.0%
	B2		Fine-grained conglomerates and conglomeratic sandstones. Clay chips	Low-angle cross-stratification	Bed load. Migration of asymptotic dunes	0.2 – 7	10.4%
	B2s		Medium- to coarse-grained sandstones. Abundant clay chips	Low-angle cross-stratification	Bed load. Migration of asymptotic dunes	0.2 – 1.5	15
	B3		Fine-grained conglomerates and conglomeratic sandstones. Clay chips	Diffuse horizontal lamination, Aligned clasts	Bed load. Drag and rolling	0.12 – 14.75	13.2%
	B3h		Fine-grained conglomerates and conglomeratic sandstones. Clay chips	Low-angle lamination (hummocky-like)	Bed load. Drag and rolling. Combined flow	0.2 – 3	25
Traction Plus Fallout	S1		Medium- to fine-grained sandstones	Massive, small clay chips, dish	Progressive aggradation from quasi-steady turbulent flows	0.1 – 9.5	6.8%
	S1L		Medium- to fine-grained sandstones. Discontinuous silt levels	Massive, clay chips, dish, load structures, plastic clay chips	Progressive aggradation from quasi-steady turbulent flows (levee transition)	0.1 – 3.6	18
	S2		Medium- to fine-grained sandstones	Planar lamination	Progressive aggradation from quasi-steady turbulent flows	0.1 – 3	3.3%
	S2h		Medium- to fine-grained sandstones	Low-angle lamination (hummocky-like)	Progressive aggradation from quasi-steady flows (combined flows)	0.1 – 1.5	3.3%
	S2L		Fine-grained sandstones. Levels of silts and plant debris	Planar lamination	Progressive aggradation from quasi-steady turbulent flows (levee transition)	0.1 – 0.3	3.3%
	S3		Fine-grained sandstones	Climbing ripples	Traction plus fallout in quasi-steady turbulent flows	0.1 – 0.3	8
Lofting	L		Fine-grained sandstones and siltstones, plant debris, and micas	Massive to laminated	Fallout from lofting plumes	0.1 – 6	3.4%
	P		Fine-grained sandstones and mudstones	Massive to laminated. Highly bioturbated	Fallout (offshore/prodelta - shoreface)	0.1 – 0.3	15

**FIGURE 10.** Main characteristics of the sedimentary facies identified in the Merecure Formation from core studies. The column on the right shows the average porosity measured for each facies. The number in the lower right corner indicates the maximum value of porosity for all samples. The number of analyses conducted for each facies is indicated in the lower left.

Individual sandstone bodies can be up to 10 m (33 ft) thick and are arranged into different hierarchical orders. Facies analysis suggests an origin related to the accumulation from sustained and long-lived turbulent flows derived from subaerial discharges (hyperpycnal flows) in a shelfal marine setting.

The analysis of the relative abundance of B, S, and L facies allowed the definition of Pt and Lt facies indices for facies prediction (Zavala et al., 2007b, 2008a).

#### *Analysis of Genetic Indices in the Merecure Formation*

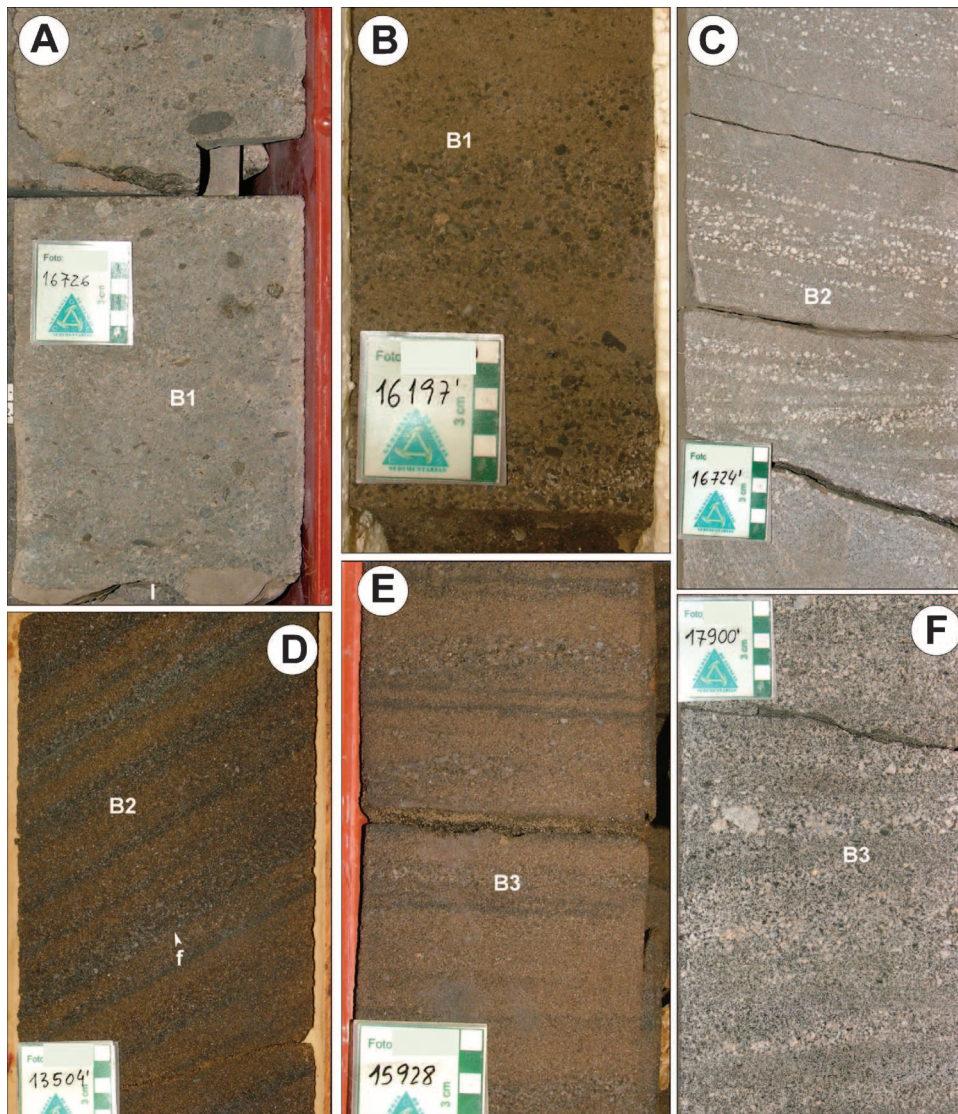
The description and classification of core facies was performed according to the genetic facies tract illustrated in Figure 5 using Excel spreadsheets especially designed for this project. Excel spreadsheets

were very useful because they allowed the fast calculation of the total thickness of the different facies categories under study. The thickness of B, S, and L facies, and the corresponding determination of the Pt and Lt facies indices, were done within the proposed sequence-stratigraphic framework. The use of a sequence-stratigraphic framework allowed the step-by-step analysis of deposition of the entire succession.

The genetic facies tract description was used in construction of genetic facies logs, which were integrated with lithologic electric logs (gamma ray [GR], neutron log [NPHI], and density log [RHOB]; Figure 13). This step was crucial to determine if the core thicknesses were representative to characterize each sequence, whether or not it was cored.

In general, the genetic facies log shows a direct correspondence with the GR log. The lowest GR values





**FIGURE 11.** The B-type facies in the Merecure Formation. (A, B) Massive fine-grained conglomerates and coarse-grained sandstones with imbricated clasts (facies B1). (C, D) Coarse-grained sandstones and fine-grained conglomerates with low-angle and asymptotic cross-bedding, interpreted as foreset (f) lamination of migrating dunes (facies B2). (E, F) Coarse-grained deposits with levels of aligned clasts (facies B3) related to bed-load processes at the base of an overpassing turbulent flow. Black and white boxes in the scale bar are 5 mm each.

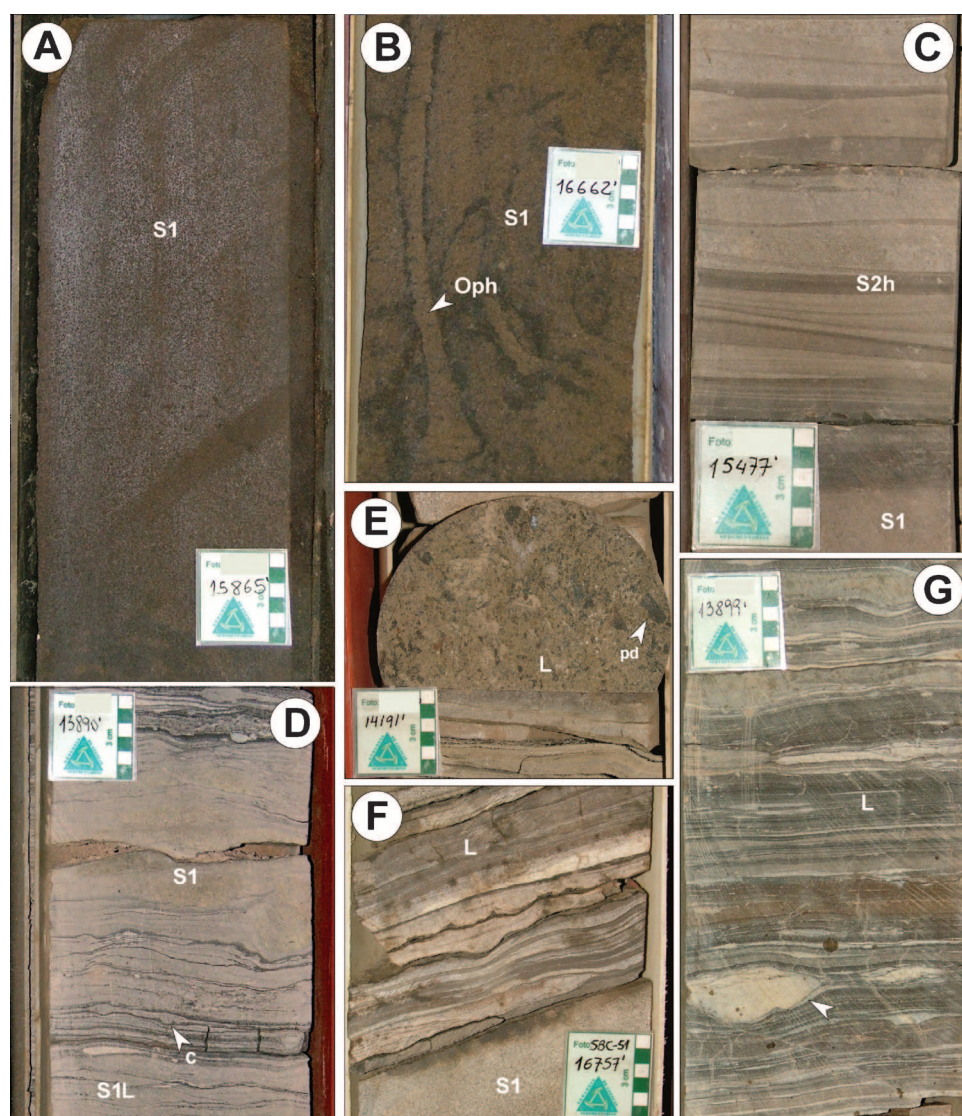
characterize type B facies. Consequently, in cases where the analyzed core interval was not considered representative or in intervals lacking core, the Pt and Lt indices were estimated from the GR log shape of the nearest wells having core data in the same interval.

Table 1 shows the final Pt and Lt indices calculated for each depositional sequence in the 30 analyzed wells. White boxes display data calculated using long cores, which are considered most representative of the sequence. The yellow boxes contain data from cores having a recorded thickness that is not considered representative and consequently has been adjusted by comparison with adjacent cored wells. The blue boxes contain estimates by log analysis from wells without core data.

The sedimentologic indices (Pt and Lt) were then plotted as maps for each sequence (Figure 14). Be-

cause Tertiary structural deformation has displaced the wells into different fault blocks, paleogeographic maps were constructed using Oligocene coordinates calculated from palinspastic reconstructions (Table 1). The analysis of genetic indices shows that Lt facies indices range between 3 and 42. An Lt facies index greater than 35 suggests the local occurrence of tectonically uplifted areas (Figure 6). Proximal indices range from 73 to 30 and suggest a proximal-to-medial position along the depositional profile (Figure 6). The analysis of genetic indices revealed that the Merecure Formation could be more extensive than previously considered, with a main sediment source from cratonic areas located toward the south and southeast (Figure 14). Mapping of the lateral facies and proximal indices suggests the existence of at least three zones of clastic input, which persist with some variations for the three identified sequences.





**FIGURE 12.** The S- and L-type facies in the Merecure Formation. (A, B) Massive fine-grained sandstones (facies S1) deposited from sustained turbulent flows. Note in panel B the *Ophiomorpha* burrows (Oph), which are interpreted as doomed pioneers. (C) Fine-grained sandstones with small-scale hummocky cross-stratification (facies S2h). (D) Massive fine-grained sandstones (facies S1) interbedded with carbonaceous levels (c) with micas (facies S1L) deposited in the flow transition zone. (E, F, G) Thin intercalations of fine-grained sandstones and siltstones with abundant plant debris (pd) and micas (facies L) deposited at flow margins. Sandstone levels show load structures (arrow) indicating soft sediment deformation. Bioturbation is scarce and characterized by rare *Palaeophycus*. Black and white boxes in the scale bar are 5 mm each.

These zones of clastic supply are located toward the southwest, south, and southeast.

Index mapping also suggests a syntectonic accumulation during the Oligocene, which controlled the subaqueous topography and the distribution of sandstone bodies. Figure 15 shows a possible depositional scenario for the accumulation of the hyperpycnal deposits of the Merecure Formation.

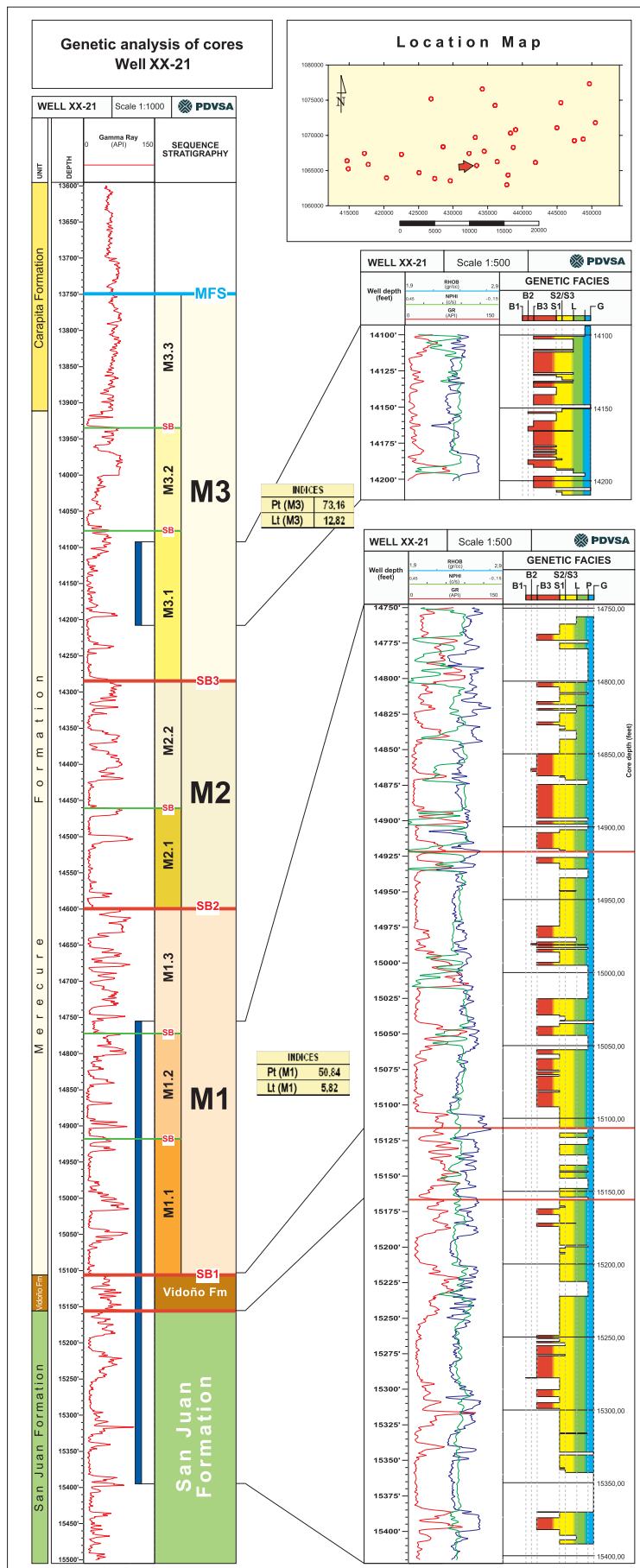
Petrographic data and conventional analysis of rock samples suggest a close relation between reservoir properties and facies. The B facies types show the best overall petrophysical properties, with porosities up to 25% (Figure 10). The S1 facies have good porosities related to their original open packing, but permeability is reduced by compaction and infiltration of fine-grained materials into pore spaces. In decreasing order of petrophysical quality, the best facies are the B3, followed by facies B2, B1, S1, L,

and S2–S3. As B-type facies have the best petrophysical properties, the facies maps of Figure 14 can be used to predict reservoir quality in undrilled areas, with an important role in diminishing risks of new ventures.

## CONCLUSIONS

The application of geographically controlled sedimentologic indices to quantify the relationships between hyperpycnal-flow-related facies has proven to be a very useful technique in the analysis of Merecure Formation reservoir strata.

When analyzed in the context of a genetic facies tract, hyperpycnal-flow-related facies have characteristics that allow the quantification of geographically controlled depositional processes, which can be determined from field and core studies. The determination



**FIGURE 13.** Example of a sedimentologic sheet used for the genetic indices analysis. The log on the left shows the cored intervals (purple bars), which are displayed on the genetic facies log of the right. SB = sequence boundary; MFS = maximum flooding surface; Fm = Formation; Gr = gamma ray; NPHI = neutron log; RHOB = density log.

**Table 1.** Calculated (white), corrected (yellow) and estimated (blue) proximal (Pt) and lateral facies (Lt) indices of the M1, M2 and M3 sequences in the analyzed wells. The two columns on the right display the coordinates during the Oligocene calculated from palinspastic reconstructions.

WELL	Pt (M1)	Lt (M1)	Pt (M2)	Lt (M2)	Pt (M3)	Lt (M3)	R COORD X	R COORD Y
1	46.67	5.36	60.61	18.01	71.72	7.82	413492.38	1078465.55
2	46.67	6.00	61.00	18.01	72.00	7.82	413603.66	1078141.77
3	54.00	14.00	45.00	16.00	72.00	8.00	416417.68	1077624.09
4	53.85	9.00	45.00	16.00	65.00	8.00	419190.85	1074409.15
5	55.00	15.00	51.05	26.28	60.00	9.00	415822.87	1080796.65
6	26.88	43.01	47.67	10.85	37.99	13.08	420742.38	1085084.76
7	no well log		61.00	18.00	59.89	5.68	426878.66	1084021.65
8	58.54	25.90	56.32	11.00	55.00	8.00	423085.37	1082084.76
9	36.03	3.58	55.00	10.00	51.00	10.00	425316.46	1080330.49
10	37.66	6.00	60.00	10.00	48.00	10.00	427487.20	1079065.85
11	45.00	12.00	40.00	24.00	29.52	15.00	425020.12	1090661.59
12	50.00	10.00	56.00	11.00	73.39	9.00	434077.44	1092925.61
13	50.00	10.00	56.00	10.00	73.39	9.55	431722.56	1095463.11
14	55.00	10.00	40.00	24.00	39.39	16.80	431499.00	1086249.00
15	68.37	11.04	52.07	14.38	38.52	5.67	436962.20	1089980.79
16	60.98	6.32	52.00	14.00	30.00	20.00	436923.17	1088394.51
17	63.72	17.92	52.00	12.00	35.00	8.00	437112.80	1086606.71
18	45.00	15.00	43.00	24.00	40.00	12.00	430703.96	1081758.84
19	62.71	8.21	55.00	20.00	65.00	12.00	434398.48	1083513.41
20	62.52	4.08	40.62	24.48	63.47	12.58	432556.10	1084565.55
21	50.84	5.82	50.00	11.00	73.16	12.82	432181.10	1081875.91
22	41.33	4.36	56.00	10.00	65.00	9.30	435728.66	1080481.71
23	60.00	10.00	75.60	2.79	65.00	9.30	435892.99	1082344.51
24	55.00	15.00	74.60	9.15	38.85	6.08	439954.27	1084228.66
25	62.00	7.00	64.96	0.00	82.00	3.88	442880.18	1089617.99
26	62.90	7.20	79.00	2.16	90.00	3.78	445299.09	1087482.01
27	62.19	11.27	81.98	5.29	83.67	3.59	446577.13	1087885.06
28	60.18	8.10	48.18	6.81	55.50	1.66	448351.22	1091022.26
29	60.00	8.00	58.36	7.00	80.00	2.00	444580.49	1094153.35
30	30.00	7.00	58.00	7.00	0.00	3.00	448890.55	1101730.18

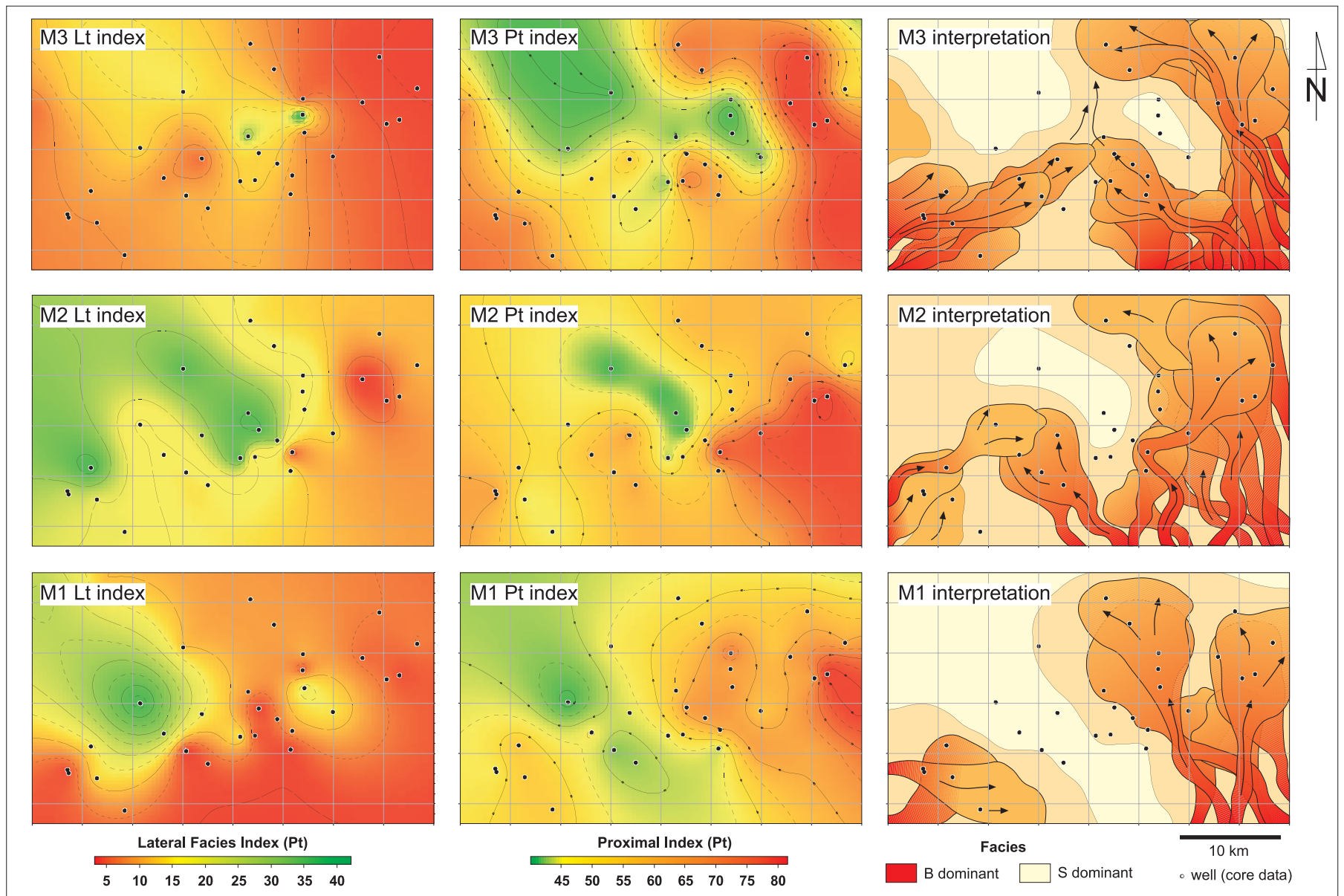
and mapping of Pt and Lt indices allow prediction of facies distribution, source area, topographic controls on sedimentation, and when integrated with petrophysical analysis, reservoir quality.

The genetic indices procedure described in this chapter was exclusively developed for the analysis of hyperpycnal systems. Consequently, the interpretation of a hyperpycnal system as the main depositional system must first be documented by careful and detailed conventional facies analysis. In addition, the analysis of genetic indices must be done within a sequence-stratigraphic framework to iden-

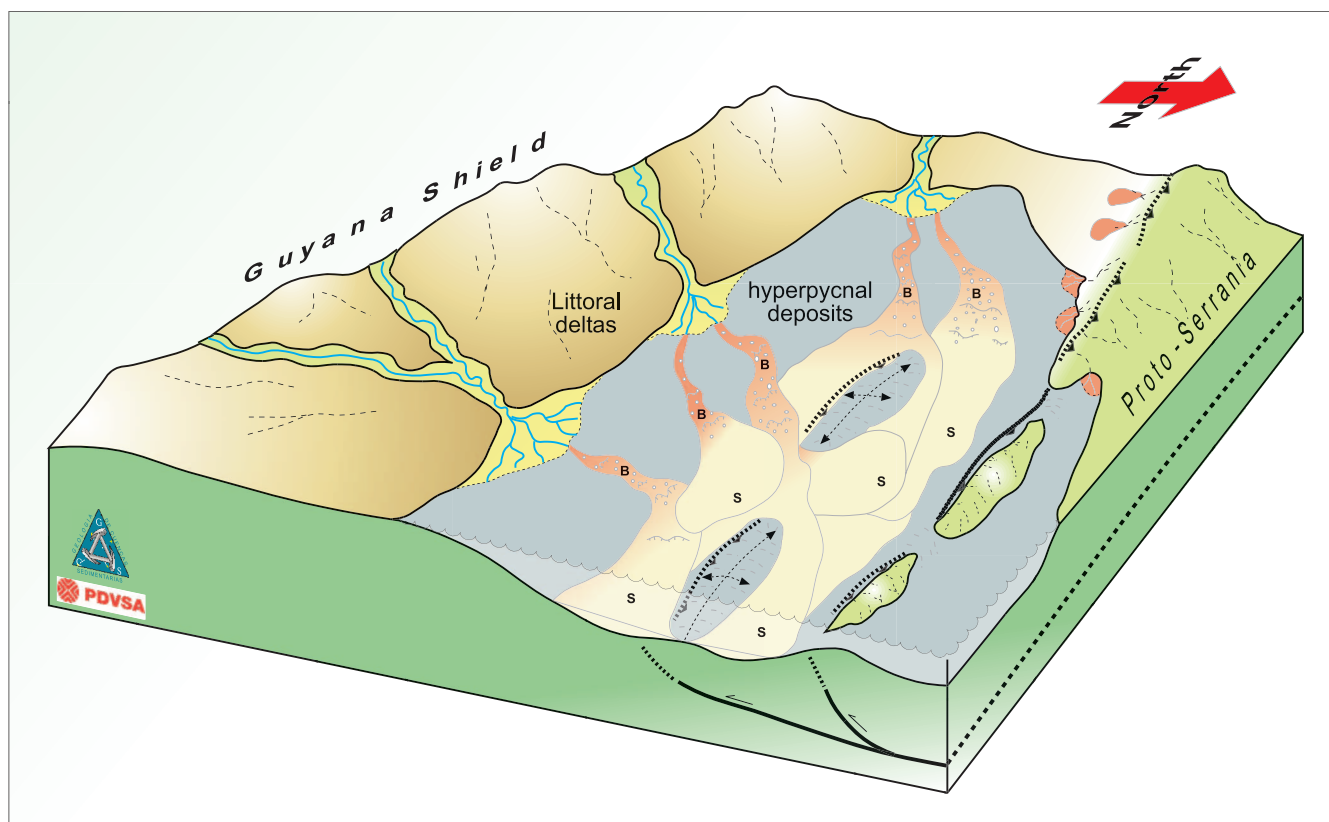
tify strata from the same stratigraphic (coeval) interval. It is necessary to point out that the genetic facies analysis and classification do not replace conventional core description and facies analysis, which are crucial to determine the environment of deposition. Also, it is important that cores analyzed are of representative thicknesses of the sequence studied.

Facies analysis conducted on 3876.75 m (12,718.99 ft) of Oligocene to lower Miocene Merecure Formation cores from 30 wells located in the Maturin Subbasin, Venezuela, provided the database to review its origin, facies distribution, and internal architecture. Facies





**FIGURE 14.** Lateral facies (Lt) and proximal indices maps (left) and their related interpretation (right) showing the distribution of B-type facies. Because B-type facies display the best petrophysical properties, these maps can be used as a proxy to predict the distribution of high-quality reservoirs.



**FIGURE 15.** Proposed depositional model for the accumulation of sandstone bodies of the Merecure Formation by hyperpycnal flows triggered from littoral deltas located toward the south and southwest. The accumulation of these sandstones was controlled by a subaqueous topography resulting from early growing tectonic structures associated with the “proto-serrania.”

analysis suggests that the strata were accumulated in a shelfal marine environment by long-lived turbulent flows linked to direct fluvial discharges (hyperpycnal systems). Twelve hyperpycnal-related sedimentary facies were recognized, which can be grouped into three main facies categories related to B, S, and L processes. The Pt and Lt indices for all three identified sequences (M1, M2, and M3) suggest the existence of three zones of clastic input located toward the southwest, south, and southeast, which persist with some variations for the three identified sequences. The Pt indices range from 73 to 30 and suggest for the entire system a proximal-to-medial position along the depositional profile. The Lt indices can be up to 42 in some specific areas, indicating synsedimentary growth structures that deeply controlled the location of main sandstone bodies. The analysis of the genetic indices suggests that the system may be larger than previously considered. Because in the system under study B facies types display the best petrophysics, the Pt map could be used to estimate the reservoir quality in un-drilled areas.

## ACKNOWLEDGMENTS

We thank PDVSA for permitting publication of the methodology used for the analysis of the Merecure Formation in the subsurface. Roger Slatt and an anonymous reviewer made important suggestions that substantially improved the contents of this chapter.

## REFERENCES CITED

- Bates, C., 1953, Rational theory of delta formation: AAPG Bulletin, v. 37, p. 2119–2162.
- Bouma, A. H., 1962, Sedimentology of some flysch deposits: A graphic approach to facies interpretation: Amsterdam, Netherlands, Elsevier, 168 p.
- Bourget, J., S. Zaragosi, T. Mulder, J. L. Schneider, T. Garlan, A. Van Toer, V. Mas, and N. Ellouz-Zimmermann, 2010, Hyperpycnal-fed turbidite lobe architecture and recent sedimentary processes: A case study from the Al Batha turbidite system, Oman margin: Sedimentary Geology, v. 229, p. 144–159, doi:10.1016/j.sedgeo.2009.03.009.
- Campos, V., R. Lander, and S. Cabrera, 1985, Evolución



- estructural en el noreste de Anzoátegui y su relación con el norte de Monagas: Memorias, VI Congreso Geológico, Venezolano, Caracas, Sociedad Venezolana de Geología, v. 4, p. 2397–2414.
- Cheng-Shing, C., and Y. Ho-Shing, 2008, Evidence of hyperpycnal flows at the head of the meandering Kaoping Canyon off SW Taiwan: *Geo-Marine Letters*, v. 28, p. 161–169, doi:[10.1007/s00367-007-0098-7](https://doi.org/10.1007/s00367-007-0098-7).
- Erlich, R. N., and S. F. Barrett, 1994, Petroleum geology of the eastern Venezuela foreland basin: *AAPG Memoir* 55, p. 341–362.
- Funkhouser, H. J., L. C. Sass, and H. D. Hedberg, 1948, Santa Ana, San Joaquín, Guárico and Santa Rosa oil fields (Anaco fields), central Anzoátegui, Venezuela: *AAPG Bulletin*, v. 32, p. 1851–1908.
- González de Juana, C., J. Iturralde de Arozena, and X. Picard, 1980, Geología de Venezuela y de sus Cuencas Petrolíferas: Caracas, Venezuela, Ediciones Foninves, 1021 p.
- Grimm, K. A., and K. B. Föllmi, 1994, Doomed pioneers: Allochthonous crustacean tracemakers in anaerobic basinal strata, Oligo-Miocene San Gregorio Formation, Baja California Sur, Mexico: *Palaaios*, v. 9, p. 313–334, doi:[10.2307/3515054](https://doi.org/10.2307/3515054).
- Haner, B. E., 1971, Morphology and sediments of Redondo submarine fan, southern California: *Geological Society of America Bulletin*, v. 82, p. 2413–2432, doi:[10.1130/0016-7606\(1971\)82\[2413:MASORS\]2.0.CO;2](https://doi.org/10.1130/0016-7606(1971)82[2413:MASORS]2.0.CO;2).
- Hesse, R., H. Rashid, and S. Khodabakhsh, 2004, Fine-grained sediment lofting from meltwater-generated turbidity currents during Heinrich events: *Geology*, v. 32, p. 449–452, doi:[10.1130/G20136.1](https://doi.org/10.1130/G20136.1).
- Jackson, C. A. L., and H. D. Johnson, 2009, Sustained turbidity currents and their interaction with debrite-related topography; Labuan Island, offshore NW Borneo, Malaysia: *Sedimentary Geology*, v. 219, p. 77–96, doi:[10.1016/j.sedgeo.2009.04.008](https://doi.org/10.1016/j.sedgeo.2009.04.008).
- Knapp, R. T., 1943, Density currents: Their mixing characteristics and their effect on the turbulence structure of the associated flow: *Proceedings of the Second Hydraulics Conference*, Bulletin 27, University of Iowa Studies in Engineering, p. 289–306.
- Kneller, B., and M. Branney, 1995, Sustained high-density turbidity currents and the deposition of thick massive sands: *Sedimentology*, v. 42, p. 607–616, doi:[10.1111/j.1365-3091.1995.tb00395.x](https://doi.org/10.1111/j.1365-3091.1995.tb00395.x).
- Kneller, B., and C. Buckee, 2000, The structure and fluid mechanics of turbidity currents: A review of some recent studies and their geological implications: *Sedimentology*, v. 47, p. 62–94, doi:[10.1046/j.1365-3091.2000.047s1062.x](https://doi.org/10.1046/j.1365-3091.2000.047s1062.x).
- Lamb, M. P., and D. Mohrig, 2009, Do hyperpycnal-flow deposits record river-flood dynamics?: *Geology*, v. 37, p. 1067–1070, doi:[10.1130/G30286A.1](https://doi.org/10.1130/G30286A.1).
- Lamb, M. P., P. M. Myrow, C. Lukens, K. Houck, and J. Strauss, 2008, Deposits from wave-influenced turbidity currents: Pennsylvanian Minturn Formation, Colorado: *Journal of Sedimentary Research*, v. 78, p. 480–498, doi:[10.2110/jsr.2008.052](https://doi.org/10.2110/jsr.2008.052).
- Lovell, J. P. B., 1969, Tyee Formation: A study of proximity in turbidites: *Journal of Sedimentary Petrology*, v. 39, p. 935–953.
- Lovell, J. P. B., 1970, The palaeogeographical significance of lateral variations in the ratio of sandstone to shale and other features of the Aberystwyth Grits: *Geological Magazine*, v. 107, p. 147–158, doi:[10.1017/S0016756800055503](https://doi.org/10.1017/S0016756800055503).
- Macdonald, D. I. M., 1986, Proximal to distal sedimentological variation in a linear turbidite trough: Implications for the fan model: *Sedimentology*, v. 33, p. 243–259, doi:[10.1111/j.1365-3091.1986.tb00534.x](https://doi.org/10.1111/j.1365-3091.1986.tb00534.x).
- McCabe, P. J., and B. Waugh, 1973, Wenlock and Ludlow sedimentation in the Austwick and Horton-in-Ribblesdale Inlier, NW Yorkshire: *Proceedings of the Yorkshire Geological Society*, v. 39, p. 445–470.
- Mulder, T., and J. Alexander, 2001, The physical character of subaqueous sedimentary density flows and their deposits: *Sedimentology*, v. 48, p. 269–299, doi:[10.1046/j.1365-3091.2001.00360.x](https://doi.org/10.1046/j.1365-3091.2001.00360.x).
- Mulder, T., and J. P. M. Syvitski, 1995, Turbidity current generated at river mouths during exceptional discharges to the world oceans: *Journal of Geology*, v. 103, p. 285–299, doi:[10.1086/629747](https://doi.org/10.1086/629747).
- Mulder, T., J. P. M. Syvitski, S. Migeon, J. C. Faugères, and B. Savoye, 2003, Marine hyperpycnal flows: Initiation, behavior and related deposits, A review: *Marine and Petroleum Geology*, v. 20, p. 861–882, doi:[10.1016/j.marpetgeo.2003.01.003](https://doi.org/10.1016/j.marpetgeo.2003.01.003).
- Mutti, E., and W. R. Normark, 1987, Comparing examples of modern and ancient turbidite systems: Problems and concepts, in J. K. Leggett and G. G. Zuffa, eds., *Marine clastic sedimentology: Concepts and case studies*: London, Graham and Trotman, p. 1–38.
- Mutti, E., and F. Ricci Lucchi, 1972, Le torbiditi dell'Appennino Settentrionale: Introduzione all'analisi di facies: *Memorie della Società Geologica Italiana*, v. 11, p. 161–199.
- Mutti, E., and M. Sonnino, 1981, Compensation cycles: A diagnostic feature of turbidite sandstone lobes (abs.): Bologna, Italy, 2d European Regional Meeting of International Association of Sedimentologists, p. 120–123.
- Mutti, E., G. Davoli, R. Tinterri, and C. Zavala, 1996, The importance of ancient fluvio-deltaic systems dominated by catastrophic flooding in tectonically active basins: *Memorie di Scienze Geologiche*, Università di Padova, Padova, Italy, v. 48, p. 233–291.
- Mutti, E., N. Mavilla, S. Angella, and L. Fava, 1999, An introduction to the analysis of ancient turbidite basins from an outcrop perspective: *AAPG Continuing Education Course Note* 39, p. 1–98.
- Mutti, E., R. Tinterri, G. Benevelli, D. Di Biase, and G. Cavanna, 2003, Deltaic, mixed and turbidite sedimentation of ancient foreland basins: *Marine and Petroleum Geology*, v. 20, p. 733–755, doi:[10.1016/j.marpetgeo.2003.09.001](https://doi.org/10.1016/j.marpetgeo.2003.09.001).
- Mutti, E., D. Bernoulli, F. Ricci Lucchi, and R. Tinterri, 2009,

- Turbidites and turbidity currents from Alpine “flysch” to the exploration of continental margins: *Sedimentology*, v. 56, p. 267–318, doi:[10.1111/j.1365-3091.2008.01019.x](https://doi.org/10.1111/j.1365-3091.2008.01019.x).
- Nakajima, T., 2006, Hyperpycnites deposited 700 km away from river mouths in the Central Japan Sea: *Journal of Sedimentary Research*, v. 76, p. 59–72.
- Natland, M. L., and P. H. Kuenen, 1951, Sedimentary history of the Ventura Basin, California, and the action of turbidity currents, in J. L. Haugh, ed., *Turbidity currents and the transportation of coarse sediments into deep water*: SEPM Special Publication 2, p. 76–107.
- Nelson, C. H., W. R. Normark, A. H. Bouma, and P. R. Carlson, 1978, Thin-bedded turbidites in modern submarine canyons and fans, in D. J. Stanley and G. Kelling, eds., *Sedimentation in submarine canyons, fans and trenches*: Stroudsburg, Pennsylvania, Dowden, Hutchinson and Ross, p. 177–189.
- Nilsen, T. H., 1980, Modern and ancient submarine fans: Discussion of papers by R. G. Walker and W. R. Normark: *AAPG Bulletin*, v. 64, p. 1094–1101.
- Normark, W. R., and D. J. W. Piper, 1991, Initiation processes and flow evolution of turbidity currents: Implications for the depositional record, in R. H. Osborne, ed., *From shoreline to abyss: Contribution in marine geology in honor of Francis Parker Shepard*: SEPM Special Publication 46, p. 207–230.
- Parnaud, F., Y. Gou, J.-C. Pascual, I. Truskowski, O. Gallango, H. Passalacqua, and F. Roure, 1995, Petroleum geology of the central part of the eastern Venezuela Basin, in A. J. Tankard, R. S. Suárez, and H. J. Welsink, eds., *Petroleum basins of South America*: AAPG Memoir 62, p. 741–756.
- Petter, A. L., and R. J. Steel, 2005, Deepwater-slope channels and hyperpycnal flows from the Eocene of the Central Spitsbergen Basin: Predicting basin-floor sands from a shelf edge/upper slope perspective, AAPG Annual Meeting, June 19–22, 2005, Calgary, Alberta.
- Plink-Björklund, P., and R. J. Steel, 2004, Initiation of turbidite currents: Outcrop evidence for Eocene hyperpycnal flow turbidites: *Sedimentary Geology*, v. 165, p. 29–52, doi:[10.1016/j.sedgeo.2003.10.013](https://doi.org/10.1016/j.sedgeo.2003.10.013).
- Porras, J. S., E. L. Vallejo, D. Marchal, and C. Selva, 2002, Extensional folding in the eastern Venezuela basin: Examples from fields of Oritupano-Leona block: AAPG Annual Meeting Program, March 10–13, 2002, Search and Discovery Article 50003 (2003), 7 p.
- Postma, G., F. J. Hilgen, and W. J. Zachariasse, 1993, Precession punctuated growth of a late Miocene submarine fan lobe on Gavdos (Greece): *Terra Nova*, v. 5, p. 438–444, doi:[10.1111/j.1365-3121.1993.tb00281.x](https://doi.org/10.1111/j.1365-3121.1993.tb00281.x).
- Schlumberger, 1997, WEC, Venezuela, Evaluación de Pozos: Caracas, Venezuela, Schlumberger, 397 p.
- Schumm, S. A., 1977, *The fluvial system*: New York, John Wiley and Sons, 338 p.
- Schumm, S. A., 1981, Evolution and response of the fluvial system: Sedimentologic implications: SEPM Special Publication 31, p. 19–29.
- Socas, M. M., 1991, Estudio sedimentológico de la Formación Naricual, estado Anzoátegui: Tesis de Grado, Universidad Central de Venezuela, Caracas, 302 p.
- Sparks, R. S. J., R. T. Bonnecaze, H. E. Huppert, J. R. Lister, M. A. Hallworth, J. Phillips, and H. Mader, 1993, Sediment-laden gravity currents with reversing buoyancy: *Earth and Planetary Science Letters*, v. 114, p. 243–257, doi:[10.1016/0012-821X\(93\)90028-8](https://doi.org/10.1016/0012-821X(93)90028-8).
- Stainforth, R. M., 1971, La Formación Carapita de Venezuela oriental: IV Congreso Geológico Venezolano, Memoria, Boletín Geológico, Caracas, Publicación Especial 5, v. 1, p. 433–463.
- Sumner, E. J., L. A. Amy, and P. J. Talling, 2008, Deposit structure and processes of sand deposition from decelerating sediment suspensions: *Journal of Sedimentary Research*, v. 78, p. 529–547, doi:[10.2110/jsr.2008.062](https://doi.org/10.2110/jsr.2008.062).
- Walker, R. G., 1967, Turbidite sedimentary structures and their relationship to proximal and distal depositional environments: *Journal of Sedimentary Petrology*, v. 37, p. 25–43.
- Walker, R. G., 1978, Deep water sandstone facies and ancient submarine fans: Models for exploration for stratigraphic traps: *AAPG Bulletin*, v. 62, p. 932–966.
- Wynn, R. B., N. H. Kenyon, D. G. Masson, D. A. V. Stow, and P. P. E. Weaver, 2002, Characterization and recognition of deep-water channel-lobe transition zones: *AAPG Bulletin*, v. 86, p. 1441–1462.
- Zavala, C., 2008, Toward a genetic facies tract for the analysis of hyperpycnal deposits, in J. J. Ponce and E. B. Olivero, conveners, *Sediment transfer from shelf to deepwater—Revisiting the delivery mechanisms*: Conference Proceedings, AAPG Search and Discovery Article 50075, AAPG Hedberg Conference, March 3–7, 2008, Ushuaia-Patagonia, Argentina, 2 p., <http://www.searchanddiscovery.com/documents/2008/jw0805zavala/> (accessed July 15, 2011).
- Zavala, C., J. Ponce, M. Arcuri, D. Drittanti, H. Freije, and M. Asensio, 2006a, Ancient lacustrine hyperpycnites: A depositional model from a case study in the Rayoso Formation (Cretaceous) of west-central Argentina: *Journal of Sedimentary Research*, v. 76, p. 40–58.
- Zavala, C., M. Arcuri, and H. Gamero, 2006b, Toward a genetic model for the analysis of hyperpycnal systems (abs.): *Geological Society of America Abstracts with Programs*, v. 38, no. 7, p. 541.
- Zavala, C., H. Gamero, and M. Arcuri, 2006c, Lofting rhythmites: A diagnostic feature for the recognition of hyperpycnal deposits (abs.): *Geological Society of America Abstracts with Programs*, v. 38, no. 7, p. 541.
- Zavala, C., M. Arcuri, H. Gamero, and C. Contreras, 2007a, The composite bed: A new distinctive feature of hyperpycnal deposition (abs.): AAPG Annual Convention and Exhibition, v. 16, p. 157.
- Zavala, C., J. Marcano, and J. Carvajal, 2007b, Proximity and laterality indices: A new tool for the analysis of ancient hyperpycnal deposits in the subsurface: *Proceedings of the 4th Geological Society of Trinidad and Tobago Geological Conference*, 3 p.

- Zavala, C., J. Carvajal, J. Marciano, and M. Delgado, 2008a, Sedimentological indices: A new tool for regional studies of hyperpycnal systems, *in* J. J. Ponce and E. B. Olivero, conveners, Sediment transfer from shelf to deepwater—Revisiting the delivery mechanisms: Conference Proceedings, AAPG Search and Discovery Article 50076, AAPG Hedberg Conference, March 3–7, 2008, Ushuaia-Patagonia, Argentina, 4 p., <http://www.searchanddiscovery.com/documents/2008/jw0807zavala/> (accessed July 15, 2011).
- Zavala, C., L. Blanco Valiente, and Y. Vallez, 2008b, The origin of lofting rhythmites: Lessons from thin sections, *in* J. J. Ponce and E. B. Olivero, conveners, Sediment transfer from shelf to deepwater—Revisiting the delivery mechanisms: Conference Proceedings, AAPG Search and Discovery Article 50077, AAPG Hedberg Conference, March 3–7, 2008, Ushuaia-Patagonia, Argentina, 4 p., <http://www.searchanddiscovery.com/documents/2008/jw0807zavala/> (accessed July 15, 2011).
- Zavala, C., M. Arcuri, H. Gamero Diaz, C. Contreras, and M. Di Meglio, 2011, A genetic facies tract for the analysis of sustained hyperpycnal flow deposits, *in* R. M. Slatt and C. Zavala, eds., Sediment transfer from shelf to deep water—Revisiting the delivery system: AAPG Studies in Geology 61, p. 31–51.

